Mesoscopic harmonic mapping of electromechanical response in a relaxor ferroelectric

Rama K. Vasudevan,[1] Shujun Zhang,[2] Jilai Ding,[3] M. Baris Okatan,[1] Stephen Jesse,[1] Sergei V. Kalinin,[1] and Nazanin Bassiri-Gharb[3,4,a)]

[1]*Center for Nanophase Materials Sciences, Oak Ridge National Laboratory, Oak Ridge, Tennessee 37831, USA and Institute for Functional Imaging of Materials, Oak Ridge National Laboratory, Oak Ridge, Tennessee 37831, USA*

[2]*Department of Materials Science and Engineering, Materials Research Institute, Pennsylvania State University, University Park, Pennsylvania 16802, USA*

[3]*School of Materials Science and Engineering, Georgia Institute of Technology, Atlanta, Georgia 30332, USA*

[4]*G. W. Woodruff School of Mechanical Engineering, Georgia Institute of Technology, Atlanta, Georgia 30332, USA*

(Received 9 February 2015; accepted 20 May 2015; published online 1 June 2015)

Relaxor-ferroelectrics are renowned for very large electrostrictive response, enabling applications in transducers, actuators, and energy harvesters. However, insight into the dissimilar contributions (polarization rotation, wall motion) to the electromechanical response from electrostrictive strain, and separation of such contributions from linear piezoelectric response are largely ignored at the mesoscale. Here, we employ a band-excitation piezoresponse force microscopy (BE-PFM) technique to explore the first and second harmonics of the piezoelectric response in prototypical relaxor-ferroelectric $0.72Pb(Mg_{1/3}Nb_{2/3})O_3$-$0.28PbTiO_3$ (PMN-0.28PT) single crystals. Third order polynomial fitting of the second harmonic reveals considerable correlation between the cubic coefficient map and the first harmonic piezoresponse amplitude. These results are interpreted under a modified Rayleigh framework, as evidence for domain wall contributions to enhanced electromechanical response. These studies highlight the contribution of domain wall motion in the electromechanical response of relaxor ferroelectrics, and further show the utility of harmonic BE-PFM measurements in spatially mapping the mesoscopic variability inherent in disordered systems. [http://dx.doi.org/10.1063/1.4921925]

The nonlinear response to a stimulus is a feature of many heterogeneous systems consisting of domains or reorientable units and/or mobile internal interfaces (ferroelectric, ferroelastic or ferromagnetic domain walls, phase boundaries, etc.). Such is the case for ferroelectric[1] and ferromagnetic systems,[2] spin glasses, etc. In piezoelectric materials, the electromechanical response contains the contributions from the (linear) piezoelectric and (nonlinear) electrostrictive strain,[3–6] the latter of which is proportional to the square of the applied field. In relaxor systems, the electrostrictive response is usually very strong, and the resulting large electromechanical coupling has enabled their use as actuators and transducer elements in imaging and energy harvesting applications.[7–9] Doping of the relaxors with a prototypical ferroelectric, such as $PbTiO_3$, can stabilize a ferroelectric phase in the relaxor, e.g., $(1-x)Pb(Mg_{1/3}Nb_{2/3})O_3$-$xPbTiO_3$ (PMN-PT), and results in significant increase in the piezoelectric and electromechanical coefficients of the system.[10]

At the phenomenological level, the piezoelectric strain S induced in a monodomain ferroelectric crystal as a result of an applied field sinusoidal signal E_{ac} can be written as[11]

$$S = QP_S^2 + 2QP_SP_{E_{ac}} + QP_{E_{ac}}^2, \quad (1)$$

where Q is the electrostrictive coefficient, P_S is the spontaneous polarization, and P_{Eac} is the field-induced polarization. However, if domains are present in the ferroelectric material, the motion and vibration of the resulting internal interfaces may also contribute to the total strain S, and manifest as nonlinearity in both the piezoelectric and electrostrictive-like terms in Eq. (1).[12–14] As a result, through an exploration of the strain response in harmonics space, the contributions to the total strain by the electrostrictive and domain wall motion phenomena can be measured, and have been demonstrated for polycrystalline[12,13] and epitaxial films[15] previously. Although the electrostrictive nature of the PMN-based relaxor-ferroelectrics has been well studied on a macroscopic scale,[5] there are few studies at the local scale at which the disorder in this system typically manifests, and much remains unclear about spatial variability of the intrinsic and extrinsic electrostrictive contributions, and their interplay with the chemically heterogeneous nanoregions, nanopolar regions, elastic clamping effects, etc., that define the complexity of the relaxor-ferroelectric.[16]

Here, we utilize a band-excitation piezoresponse force microscopy (BE-PFM) technique to explore the first and second order harmonics of the piezoresponse (field-induced strain) in the prototypical relaxor-ferroelectric PMN-0.28PT single crystals. The results reveal that the second harmonic signal appears at and above $V \sim 0.7V_{ac}$. In contrast, the first harmonic is evident at the lowest applied ac voltage. Further, third-order polynomial fitting of the second harmonic reveals that the spatial variation of the cubic fitting term correlates with the first harmonic of the piezoresponse. These results are interpreted in the framework of (intrinsic) electrostrictive

a)E-mail: nazanin.bassirigharb@me.gatech.edu

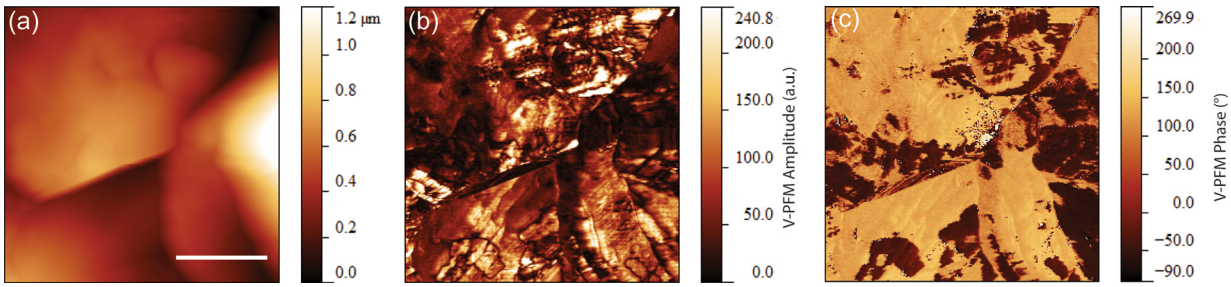

FIG. 1. Topography and Piezoresponse Force Microscopy of PMN-0.28PT. (a) Topography, (b) vertical PFM amplitude, and associated (c) phase. The scale bar in (a) is 1 μm.

and extrinsic contributions to the piezoresponse, and show the utility of BE-PFM spectroscopic methods in spatially mapping the contributions to strain in the relaxor-ferroelectrics.

The [100] oriented PMN-0.28PT single crystals were grown using the Bridgeman method and are nominally close to the morphotropic phase boundary of the PMN-PT system. A suitable piece was then diamond saw-cut, but not polished, as polishing may introduce artifacts in the ferroelectric domain structure.[17] The sample was mounted onto a puck with silver paste, which served as a counter electrode and was grounded with respect to the biased PFM tip for the BE-PFM experiments. BE-PFM experiments were performed on an Asylum Research Cypher instrument with PXi-based electronics and in-house scripts written in Matlab and Labview. More details on the harmonics BE-PFM technique can be found elsewhere.[18,19] Briefly, the spectroscopic measurement results in the piezoresponse (including the amplitude, phase, resonance, and quality factor) at a particular *(x,y)* location as a function of applied AC voltage (V_{ac}), in this case ranging from 0.09 V to 3 V. The measurements are repeated across a grid of points (60 × 60) to map the response across the surface. A second round of measurements across the same grid is subsequently preformed in order to acquire the second harmonic of the piezoresponse (by utilizing half-harmonic excitation[19]).

The topography and single frequency vertical PFM amplitude and phase of a 3 μm × 3 μm region are shown in Figs. 1(a)–1(c), and reveal that the surface is considerably rough due to the lack of polishing. The PFM amplitude and phase images confirm the presence of ferroelectric domains in the sample as evidenced by the zero amplitude lines demarcating the domain walls in Fig. 1(b) and the contrast in the phase image (Fig. 1(c)).

The first order harmonic amplitude map (at $V_{ac} = 3$ V) is shown in Fig. 2(a) and presents considerable spatial variability, while the resonance map in Fig. 2(b) shows the stiffness of the tip-surface contact varying across the surface as a result of variations in elastic clamping and surface topography. Clear correlation between the resonance map and the

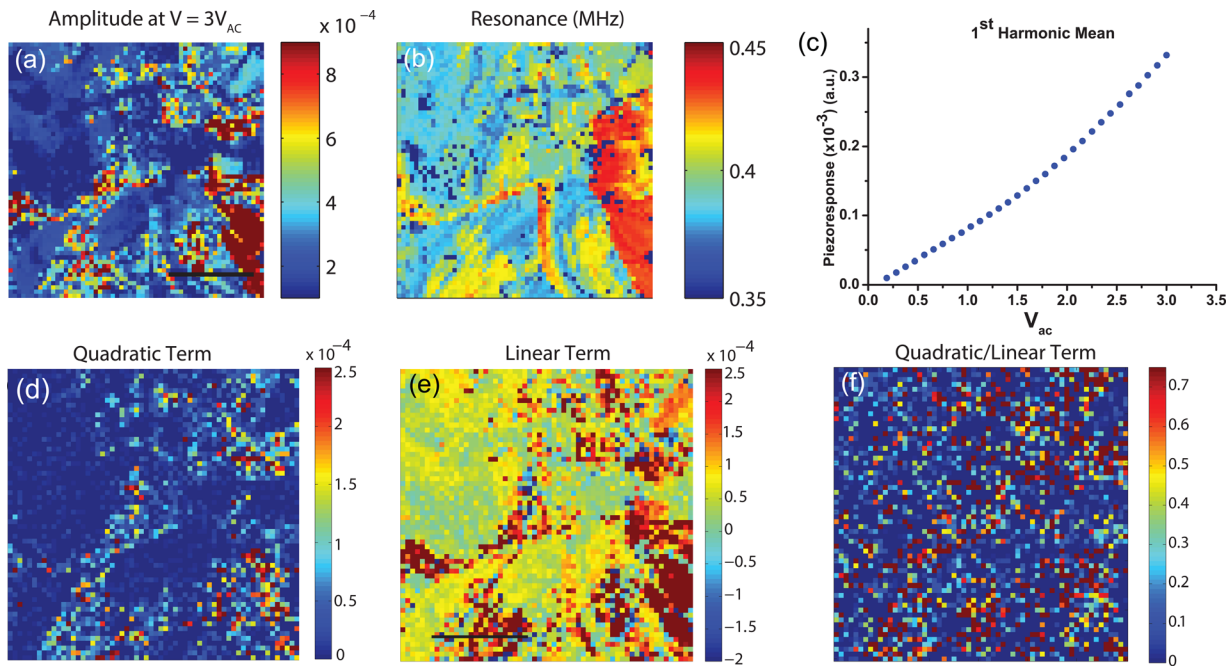

FIG. 2. First harmonic BE-PFM spectroscopy. (a) Spatial map of amplitude at $3V_{ac}$ is shown in this figure. The scale bar is 1 μm. (b) The resonant frequency map (at $3V_{ac}$) showing the variations in the stiffness of the tip-surface contact across the same region. The average response of the first harmonic piezoresponse (from all 3600 measurements) is plotted in (c). After 2nd order polynomial fitting at each *(x,y)* point in the grid, spatial maps of (d) quadratic and (e) linear terms can be produced. The ratio of quadratic to linear terms is shown in (f).

first harmonic maps are limited, and indeed should be minimal based on the reduced topographical crosstalk in band excitation approaches.[20] Any remaining correlations may be ascribed to the effect of changing elastic boundary conditions on the local piezoresponse, especially at specific microstructural features (such as topographic edges). The mean of the 1st harmonic response across the 60 × 60 grid (i.e., 3600 distinct measurements) is plotted in Fig. 2(c), and shows a slight curvature well, which is an evidence of nonlinearity. The piezoresponse displacement amplitude (hereafter termed "piezoresponse"), $A = A(x,y,V_{ac})$ was then fit to a quadratic polynomial $(a + bV_{ac} + cV_{ac}^2)$ at each (x,y) location yielding spatial maps of the quadratic and linear fitting parameters, $a = a(x,y)$ and $b = b(x,y)$, and the $c = c(x,y)$, respectively. The spatial maps for the quadratic and linear terms are plotted in Figs. 2(d) and 2(e), respectively. To obtain a quantitative measure of the nonlinear piezoresponse and its variation across the surface, we plotted the (c/b), i.e., the quadratic coefficient divided by the linear coefficient in Fig. 2(f). Larger values of this ratio correspond to increasing non-linear behavior, and can be linked to irreversible domain wall and eventual phase boundary motion in ferroelectrics, notably as the irreversible to reversible Rayleigh parameters ratio.[21–24] As seen in the mean piezoresponse in Fig. 2(c), this ratio is in general low and the curvature is small, indicating mostly linear piezoelectric behavior. Higher values can be seen at some topographic edge regions, e.g., top-right corner, presumably because elastic clamping is reduced at these sites.

The second harmonic of the piezoresponse was then measured across the same *(x,y)* spatial grid and area. While the first harmonic probes the full electromechanical response of the system, the second harmonic measures the contributions to the response arising from electrostriction as well as eventual reversible and irreversible domain wall motion present.[13,14] The amplitude of the piezoresponse's second order harmonic at $V_{ac} = 3$ V is plotted in Fig. 3(a). The second harmonic's amplitude map differs from the first harmonic amplitude, confirming that this experiment does indeed measure a different contribution to the strain than the first harmonic. However, there is some correlation (and is expected) between the two maps, as the second order contribution is a subset of the overall electromechanical response measured through the first harmonic signal. In addition, both maps appear somewhat correlated with the domain structure (Fig. 1(c)). Such behavior may be due to asymmetry in the (ferroelectric switching) potential wells, caused by preferential segregation of defects or growth processes for the crystal, leading to a preferential polarization direction(s) with respect to others. It should be noted that the single crystal solid solution has a preferential growth direction growth along [111], and is slowest along [100], which can lead to radially inhomogeneous segregation of defects at mesoscopic scales. The average second harmonic response, graphed in Fig. 3(b), shows that the response is measurable only above ~0.75 V (compare with first harmonic in Fig. 2(b)), likely due to signal comparable with the noise floor below this threshold value. However, the average response is high in amplitude and comparable to the first harmonic, especially at higher excitation signal amplitudes. This can either be due to large electrostriction, or significant contribution from domain walls in the probed volume by the tip.

For a purely electrostrictive contribution, the 2nd order harmonic piezoresponse will be well represented by $A(x,y,V) = b + cV^2$, i.e., there will be a squared dependence on the applied bias (i.e., field), with an offset due to instrumental sources. On the other hand, domain wall motion in ferroelectrics can result in both quadratic $(a + bE_0 + cE_0^2)$ as well as cubic dependencies on the applied field, and therefore, we expect such a relationship to hold in this case.[14] If there is no domain wall contribution, it would be expected that the higher order polynomial fits would not substantially improve the fitting of the piezoresponse function. As a measure of the applicability of the fitting function, we use the sum of squared errors (SSE) metric, defined as

$$SSE = \sum_{i=1}^{n} (y_i - f(V_i))^2,$$

where y_i is the piezoresponse amplitude at voltage step i for a particular (x,y) point and $f(V_i)$ is the predicted value of y_i based on the model $f(V)$ chosen. Here, the chosen functions are $f(V) = b + cV^2$, $f(V) = a + bV + cV^2$, and $f(V) = a + bV + cV^2 + dV^3$, and the result of the SSE as a function of the three functional forms are plotted in Figs. 4(a)–4(c). The results highlight the overriding electrostrictive response at the majority of the points, and can be expected for the highly electrostrictive relaxor-ferroelectrics such as PMN-PT, since there is not a large degree of change between the SSE maps in Fig. 4(a)–4(c).

After fitting the second harmonic response to a cubic polynomial at each (x,y) point, the spatial maps for the coefficients were extracted and are plotted in Figs. 4(d)–4(f) for the cubic, quadratic, and linear terms. From basic arguments,

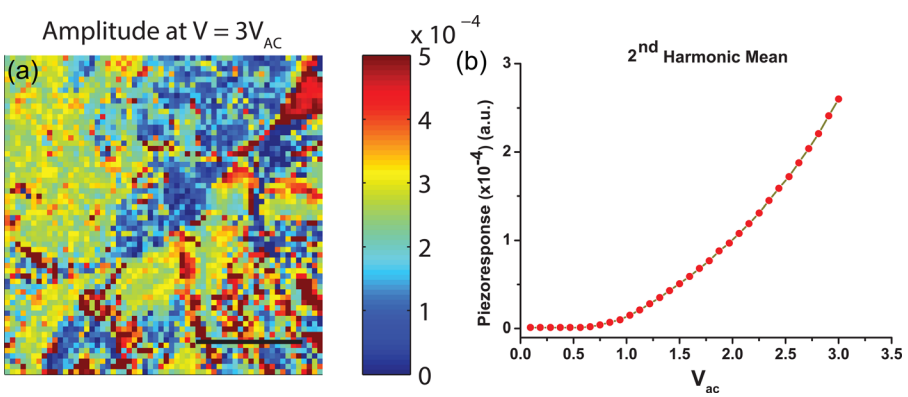

FIG. 3. Second Harmonic Results. (a) Spatial map of the second harmonic piezoresponse at $3V_{ac}$. (b) mean 2nd harmonic response (from all measured points).

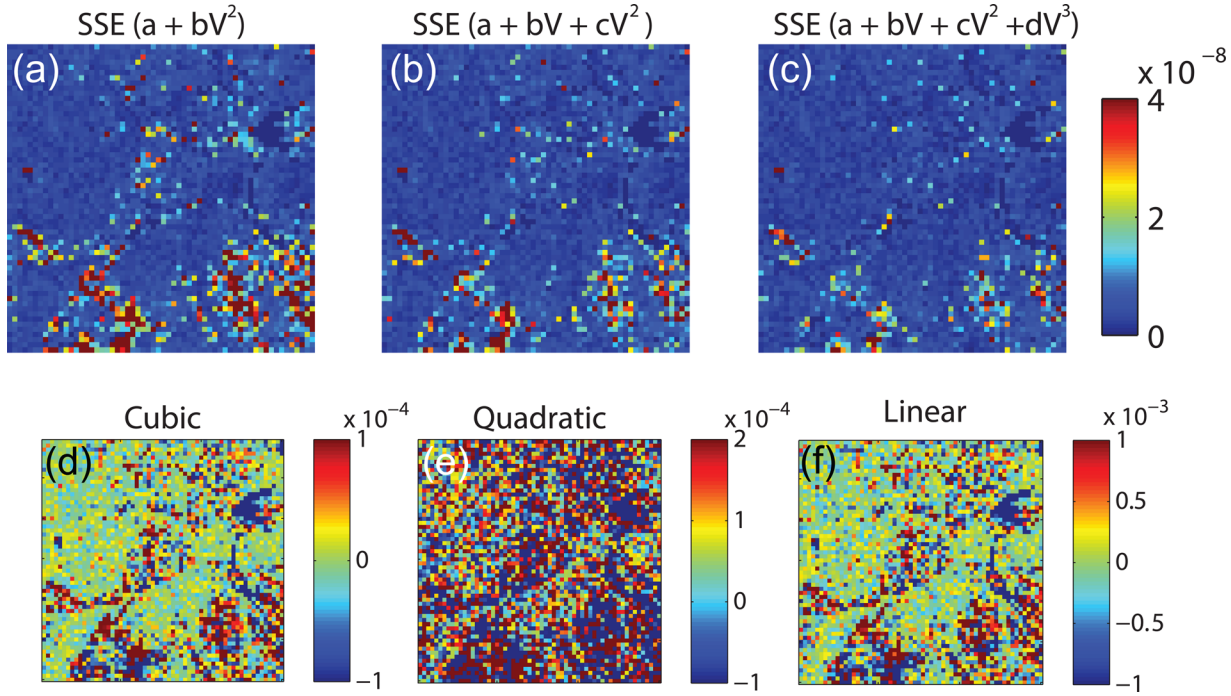

FIG. 4. SSE for (a) purely V^2 dependence, (b) quadratic (V^2+V) dependence, and (c) cubic (V^3+V^2+V) dependence. A third order polynomial fit at each (x,y) point was carried out, and the coefficients for the cubic, quadratic and linear coefficients are shown in the spatial maps in (d)–(f).

Bassiri-Gharb *et al.*[14] showed that the contribution of domain walls could indeed result in a cubic field dependence of the second harmonic for the measured strain S, i.e.,

$$S_{2\omega}(E_{ac}) = \frac{1}{8}Q\varepsilon_0^2E_0^2\left(4(\chi_{lat}+\chi_{rev})^2+8\alpha(\chi_{lat}+\chi_{rev})E_0 + 3\alpha^2E_0^2\right)\cos(2\omega) - \frac{16}{15\pi}Q\varepsilon_0^2E_0^3 \times(\chi_{lat}+\chi_{rev}+\alpha E_0)\sin(2\omega) + \text{higher order terms}, \quad (2)$$

where $E_{ac} = E_0\sin(\omega t)$ is the applied field, χ_{rev} is the reversible Rayleigh parameter for the dielectric response, χ_{lat} is the dielectric susceptibility of the lattice, and α is the irreversible Rayleigh coefficient. Equation (2) indicates that both reversible and irreversible motion of internal interfaces can produce cubic (and even quadratic) field dependencies. These dependencies arise from the dielectric nonlinearity and the coupled response of adjacent domains, which are modulated by elastic and/or electric fields. Interestingly, there is a correlation (~0.10) between the cubic coefficient map in Fig. 4(d) and the first harmonic response in Fig. 2(a), suggesting that domain wall and/or phase boundary motion (both reversible and irreversible) is a contributor to the enhanced electromechanical response in this material. That is, there is significant response modulation across the domain walls (or phase boundaries) through dielectric nonlinearity and coupled responses of adjacent domains. Indeed, if this was not the case, then the correlation of the cubic coefficient with the first harmonic spatial map should be weak or non-existent, as any internal interface motion (which would vary spatially due to defects, different degrees of clamping, chemical heterogeneities, etc.) would be completely overwhelmed by the pre-dominant electrostrictive response. Nonetheless, this analysis also proves that for the majority of points, the cubic coefficient is rather small (particularly in the terraces), and the motion of internal interfaces appears to be enhanced only near the topographic edges. It is to be noted that this work complements the macroscopic investigations of these crystals by Li *et al.*,[10] which found that there was a small but significant (~10%) contribution from irreversible domain wall displacement to the piezoelectric activity of the PMN-PT single crystal.

Finally, it is to be noted that within the current limitations of this technique, we are unable to separate polarization rotation from reversible domain wall motion, as both mechanisms contribute to the reversible part of dielectric and piezoelectric nonlinearity and are therefore intrinsic. While it may be possible to separate these contributions through analysis of field dependencies at higher harmonics, the signal was too weak in this instance to draw conclusions. However, such higher harmonic response has been previously reported for other material systems,[13] and we expect that future tool enhancements[25] will enable these measurements and therefore the underlying mechanisms.

In summary, we have used a spectroscopic harmonics-based BE-PFM method to study the mesoscopic variability of the electrostrictive-like contributions to the strain in the relaxor-ferroelectric PMN-0.28PT system. The results reveal that a significant proportion of the strain response arises from the second harmonic, which consists of electrostriction and domain wall motion. By determining the field dependencies of the piezoresponse for the second harmonic, it is shown that although the majority of the sample displays mostly pure electrostriction, motion of internal interfaces is enhanced around topographic edges and can impact the electromechanical response at these sites. These studies highlight the critical role that electrostriction and domain wall motion play in enhancing the electromechanical response of relaxor-ferroelectrics. Furthermore, such harmonic studies in

conjunction with multivariate statistical analysis can be extended to a wealth of disordered and heterogeneous systems to reveal fundamental insights at the level at which the disorder routinely manifests, i.e., in the mesoscopic regime.

This research was sponsored by the Division of Materials Sciences and Engineering, BES, DOE (RKV, SVK). A portion of this research was conducted at and partially supported by (SJ, MBO) the Center for Nanophase Materials Sciences, which is a DOE Office of Science User Facility. N.B.G. acknowledges funding from the U.S. National Science Foundation through Grant No. DMR-1255379.

[1]K. A. Schönau, L. A. Schmitt, M. Knapp, H. Fuess, R.-A. Eichel, H. Kungl, and M. J. Hoffmann, Phys. Rev. B. **75**(18), 184117 (2007).
[2]D. L. Leslie-Pelecky and R. L. Schalek, Phys. Rev. B. **59**(1), 457 (1999).
[3]F. Li, L. Jin, Z. Xu, and S. Zhang, Appl. Phys. Rev. **1**(1), 011103 (2014).
[4]R. E. Newnham, *Properties of Materials: Anisotropy, Symmetry, Structure: Anisotropy, Symmetry, Structure* (OUP Oxford, 2004).
[5]J. Zhao, A. Glazounov, Q. Zhang, and B. Toby, Appl. Phys. Lett. **72**(9), 1048 (1998).
[6]L. E. Cross, S. J. Jang, R. E. Newnham, S. Nomura, and K. Uchino, Ferroelectrics **23**(1), 187 (1980).
[7]S. Zhang, F. Li, J. Luo, R. Sahul, and T. R. Shrout, IEEE Trans. Ultrason. Ferr. **60**(8), 1572 (2013).
[8]S. E. Park and T. R. Shrout, Mater. Res. Innovations **1**(1), 20 (1997).
[9]A. Mathers, K. S. Moon, and J. Yi, IEEE Sens. J. **9**(7), 731 (2009).
[10]F. Li, S. Zhang, Z. Xu, X. Wei, J. Luo, and T. R. Shrout, J. Appl. Phys. **108**(3), 034106 (2010).
[11]P. Delobelle, E. Fribourg-Blanc, and D. Remiens, Thin Solid Films **515**(4), 1385 (2006).
[12]N. B. Gharb, S. Trolier-McKinstry, and D. Damjanovic, J. Appl. Phys. **100**(4), 044107 (2006).
[13]S. Trolier-McKinstry, N. B. Gharb, and D. Damjanovic, Appl. Phys. Lett. **88**(20), 202901 (2006).
[14]N. Bassiri-Gharb, S. Trolier-McKinstry, and D. Damjanovic, J. Appl. Phys. **110**(12), 124104 (2011).
[15]R. K. Vasudevan, M. B. Okatan, Y. Y. Liu, S. Jesse, J. C. Yang, W. I. Liang, Y. H. Chu, J. Y. Li, S. V. Kalinin, and V. Nagarajan, Phys. Rev. B. **88**(2), 020402 (2013).
[16]A. Bokov and Z.-G. Ye, in *Frontiers of Ferroelectricity* (Springer, 2007), pp. 31.
[17]A. L. Kholkin, D. A. Kiselev, I. K. Bdikin, A. Sternberg, B. Dkhil, S. Jesse, O. Ovchinnikov, and S. V. Kalinin, Materials **3**, 4860 (2010).
[18]R. K. Vasudevan, M. B. Okatan, I. Rajapaksa, Y. Kim, D. Marincel, S. Trolier-McKinstry, S. Jesse, N. Valanoor, and S. V. Kalinin, Sci. Rep. **3**, 2677 (2013).
[19]Y. Kim, A. Kumar, A. Tselev, I. Kravchenko Ivan, H. Han, I. Vrejoiu, W. Lee, D. Hesse, M. Alexe, V. Kalinin Sergei, and S. Jesse, ACS Nano **5**(11), 9104 (2011).
[20]S. Jesse, A. Kumar, S. V. Kalinin, A. Gannepali, and R. Proksch, Microsc. Today **18**(06), 34 (2010).
[21]D. V. Taylor and D. Damjanovic, J. Appl. Phys. **82**(4), 1973 (1997).
[22]A. Pramanick, D. Damjanovic, J. E. Daniels, J. C. Nino, and J. L. Jones, J. Am. Cer. Soc. **94**(2), 293 (2011).
[23]P. Bintachitt, S. Jesse, D. Damjanovic, Y. Han, I. M. Reaney, S. Trolier-McKinstry, and S. V. Kalinin, Proc. Natl. Acad. Sci. USA **107**(16), 7219 (2010).
[24]N. Bassiri-Gharb, I. Fujii, E. Hong, S. Trolier-Mckinstry, D. V. Taylor, and D. Damjanovic, J. Electroceram. **19**(1), 49 (2007).
[25]A. Belianinov, S. V. Kalinin, and S. Jesse, Nat. Commun. **6**, 6550 (2015).